# An Integrated Flow for Predicting Radiation Effects in CubeSat Onboard Electronics

Eleonora Vacca, Corrado De Sio, Luca Sterpone
*Department of Control and Computer Engineering*
*Politecnico di Torino*
Turin, Italy
{eleonora.vacca; corrado.desio; luca.sterpone}@polito.it

***Abstract*—We introduce a simulation-driven methodology to assess the Single Event Effect (SEE) sensitivity of CubeSat electronics under mission-specific radiation environments. By combining component-level Single Event Upset (SEU) cross-section data with detailed 3D structural shielding models, our approach enables fine-grained estimation of SEE rates. Applied to the RAMSES CubeSat mission, it demonstrates that accounting for 3D analysis reduce predicted SEU rates by over 50× compared to simplified standalone models. This improved precision enhances component selection, informs shielding strategies, and streamlines fault mitigation planning, ultimately supporting cost-effective and reliable mission design.**

***Index Terms*—CubeSat, Radiation, SEE, Geant4**

## I. Introduction

CubeSats are growing in popularity for space missions due to their compact size, reduced development time, and reduced costs compared to traditional satellites. However, these advantages come with significant limitations in mass, volume, and available power. Additionally, given their safety-critical nature, reliability and radiation protection are essential. However, incorporating shielding or redundancy mechanisms to protect sensitive electronic components can significantly increase the size and weight, potentially compromising the mission's feasibility or cost-effectiveness. Thus, optimizing reliability without incurring excessive overhead is a critical challenge in CubeSat design. A fundamental step in mission development is the early evaluation of electronic device susceptibility to radiation-induced effects [1]. Traditionally, this is approached through radiation testing of the Device Under Test (DUT) in isolation, assuming direct exposure to radiation [2]. However, this method neglects the complex interactions between radiation particles and the CubeSat's structure. In practice, the surrounding materials may provide partial shielding or generate secondary particles that worsen the effects. These structural influences are rarely accounted for in conventional testing, yet they can have a profound impact on the actual in-orbit reliability of an electronic component. Given the impracticality of performing radiation tests on a fully assembled CubeSat using particle accelerators due to cost, complexity, and facility limitations, an alternative evaluation methodology is needed.

In this work, we propose a simulation-driven analysis flow to improve the accuracy of radiation-induced reliability assessments for CubeSat onboard electronic components. Our methodology integrates detailed modeling of the space radiation environment with a realistic 3D representation of the CubeSat's internal structure, enabling a comprehensive evaluation of the radiation effects on onboard devices. The process begins by characterizing the mission-specific radiation environment, accounting for orbit, mission duration, and solar activity, which influence the flux of high-energy particles. This is combined with a detailed 3D model of the CubeSat, including subsystems and structural components, to simulate particle transport, nuclear interaction and secondary particle generation. Using advanced particle transport simulations with the GEANT4 toolkit [3], we obtain spatially-resolved radiation metrics, such as particle fluence and Linear Energy Transfer (LET) spectra, at specific locations within the CubeSat. These position-dependent results reveal how the spacecraft geometry and materials modulate the radiation environment experienced by specific electronic components. Finally, we propose a more realistic estimation of the Single Event Effect (SEE) rates by correlating simulated radiation conditions with experimentally derived device cross-section data, moving beyond simplified assumptions and uniform shielding models.

As a representative case study, we apply the proposed simulation framework to the European Space Agency's Rapid Apophis Mission for Space Safety (RAMSES) [4] CubeSat, developed in collaboration with Tyvak International. Focusing on the Flight Control Module (FCM) implemented in a Zynq-7030 System-on-Chip (SoC) embedding an SRAM-based FPGA, we estimate the Single Event Upset (SEU) rate. Experimental results demonstrate that our two-tiered approach, combining structural shielding effects with component-level characterization, significantly refines the SEE rate predictions. Specifically, we observed a 51.3× reduction in the estimated SEU rate when moving from the standalone analysis to the integrated 3D configuration, highlighting the critical impact of system-level shielding.

## II. State of the Art

Reliability analysis is essential for electronic components intended for space deployment. This is due to the risk posed by high-energy particles, which can induce both transient and permanent faults in devices, potentially compromising the success of the mission. The most effective method to assess a component's radiation tolerance remains radiation testing

[2]. In these tests, components are exposed to high-energy particles, and the resulting effects are directly evaluated. However, such campaigns are costly, and only a limited number of specialized facilities worldwide offer this service. Moreover, while ideally all the onboard electronics should be tested, this is not feasible in practice due to limited budget. Therefore, predictive simulation tools are commonly employed to emulate the sensitivity of components to radiation.

Among these tools, GEANT4 is widely recognized for its accuracy, allowing detailed simulation of particle trajectories through complex material structures, including device internal geometry. Nonetheless, most state-of-the-art applications of GEANT4 focus on stand-alone components. For instance, in [5], the authors modeled three FinFET technologies down to single memory cells to evaluate soft error susceptibility under exposure to protons and alpha particles. Similarly, [6] employed GEANT4 to study Single Event Burnout (SEB) in Silicon Carbide (SiC) power MOSFETs, combining Monte Carlo simulation with proton irradiation data to analyze secondary particle generation. Similarly, authors in [7] used GEANT4 Monte Carlo simulation to evaluate neutron-induced displacement effects in Si, GaAs, GaN, and SiC technologies. In contrast, [8] incorporated a full 3D CubeSat model into GEANT4 to assess the shielding effectiveness of a high-temperature superconductor (HTS) coil. Although their study considered the system-level configuration, their analysis centered on radiation shielding performance rather than estimating SEE on internal components. Differently, we use the GEANT4 toolkit to evaluate how the external and internal structures of the CubeSat, including its subsystems, modify the radiation environment that reaches a specific target component in a mission-specific scenario. We then combine these simulation results with SEE cross-section data from standalone device radiation testing to estimate the component SEE rate as it operates within the CubeSat during the mission. This approach enables a more realistic and mission-relevant reliability assessment for space electronics.

## III. Proposed Approach

We propose a two-step approach to evaluate the radiation-induced reliability of electronic components in CubeSat missions. Firstly, we model the space radiation environment and its interaction with the satellite structure to estimate the LET at the sensitive target volume. Then, we use the LET spectrum for detailed component-level evaluation. An overview of the proposed evaluation flow is reported in Fig. 1.

### A. Mission-Specific Radiation Environment Modeling

The first step of our proposed methodology aims at estimating the radiation environment within the CubeSat in a mission-specific context. This begins with the use of the Space Environment Information System (SPENVIS) tool [9], which allows modeling of space radiation conditions based on mission orbital parameters. The user defines the type of orbit (LEO, GEO, deep space, etc.) and the solar activity, which directly influence the intensity and spectral composition of

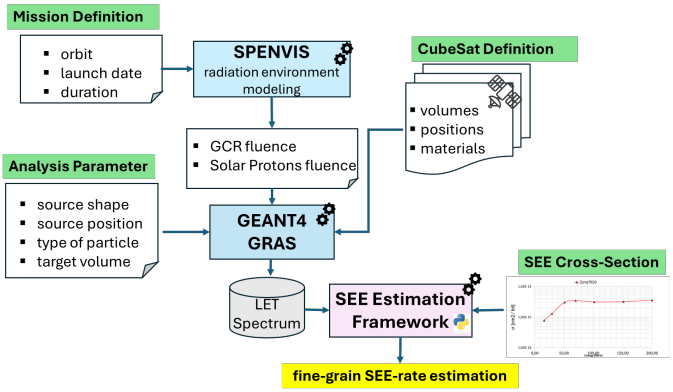


Fig. 1. Overview of the developed SEE evaluation flow

the radiation sources. The output of this analysis consists of particle fluence for protons and heavy ions, expected for the mission. To incorporate the structural and shielding effects of the spacecraft, we use GEANT4 Radiation Analysis for Space (GRAS) [10]. GRAS takes as input a Geometry Description Markup Language (GDML) file that describes the full 3D geometry of the CubeSat, including internal subsystems and materials. The radiation sources to be simulated are those defined from the SPENVIS-generated particle spectra, ensuring alignment with the actual mission conditions. Additionally, users define the shape and directionality of the radiation source, as well as the target volumes within the geometry where detailed analysis will be performed. GRAS then propagates these primary particles through the spacecraft, simulating all relevant physical interactions, such as electromagnetic and nuclear processes, thereby also generating secondary particles within the structure. For the target volume, GRAS records the energy deposited in this region by each particle track, thereby generating the LET spectrum expressed in units of MeV·cm²/mg. By observing how LET spectra vary depending on the position within the spacecraft, this approach enables the identification of shielding contributions and secondary particle production effects from neighboring subsystems. The result is a spatially-resolved, mission-tailored radiation environment inside the CubeSat, which serves as the foundation for the subsequent fine-grain analysis.

### B. Mission-Tailored Device SEE Estimation

At this stage of the analysis, although a detailed and geometry-aware LET spectrum is obtained, no direct estimation of the SEE rate is performed. Estimating the SEE rate requires combining the simulated LET spectrum with device-specific cross-section data, which are typically derived from experimental radiation test reports where the device has been exposed to accelerated particle beams. SPENVIS offers a built-in SEE rate estimation feature by allowing users to provide the device's cross-section data [11]. However, this tool accounts for shielding only as an equivalent uniform aluminum thickness, without modeling the actual spacecraft geometry or material composition. To address this limitation and enable a mission-specific spacecraft-oriented SEE evaluation, we im-

plemented a custom framework that integrates the LET spectra obtained from GRAS with the experimentally measured SEE cross-section of the device under analysis. The LET spectrum output by GRAS is structured as a histogram. On the $x$-axis are the LET bins, while on the $y$-axis are the number of particle hits. For each bin, we compute the differential fluence $\phi(\text{LET}_i)$ as follows:

$$\phi(\text{LET}_i) = \frac{N_i}{N_{\text{prim}} \cdot A} \tag{1}$$

where $N_i$ is the number of particles in bin $i$, $N_{\text{prim}}$ is the total number of primary particles simulated (up to $10^7$), and $A$ is the area of the sensitive volume in $\text{cm}^2$. This fluence represents the number of particles per $\text{cm}^2$ per unit LET that reach the target volume. The SEE cross-section $\sigma(\text{LET})$ curve of a device plots on the $y$-axis the SEE probability per sensitive node (in $\text{cm}^2$), and on the $x$-axis the LET, indicating the likelihood that a particle of a given energy will induce an SEE in the node.

Given that, the expected SEE rate for each LET bin is calculated as the product of the differential fluence and the corresponding cross-section point:

$$R_i = \phi(\text{LET}_i) \cdot \sigma(\text{LET}_i) \tag{2}$$

Summing over all bins gives the total SEU rate per bit:

$$R_{\text{SEU}} = \sum_i R_i = \sum_i \phi(\text{LET}_i) \cdot \sigma(\text{LET}_i) \tag{3}$$

This result represents the SEE rate induced by the mission-specific radiation environment as shaped by the actual CubeSat structure. If required, the rate can be normalized to a mission duration $T$ to obtain the SEU rate per bit per unit time. This methodology allows us to realistically estimate the SEU susceptibility of a specific device in its actual operational context. Unlike approaches that rely solely assume uniform shielding, our method captures both the device's physical sensitivity (through radiation test data) and the complex internal radiation environment shaped by the CubeSat geometry and material. As such, it enables a more accurate risk assessment for mission-critical components in small satellite platforms.

## IV. Experimental Analysis

The proposed SEE sensitivity evaluation methodology has been applied in the context of the ESA RAMSES space mission. RAMSES will transport two CubeSats, a lander and an orbiter, to the Apophis asteroid. This study focuses on the orbiter, a 6-unit XL CubeSat with dimensions of 13 × 24.6 × 36.6 cm. The spacecraft integrates several subsystems, each comprising multiple PCBs hosting dedicated hardware. A simplified structural model (excluding payloads) is shown in Fig. 2. Due to confidentiality constraints, the exact component locations, device types, and material details are omitted. While the proposed analysis flow has been applied to all mission-critical devices, this work presents experimental results specific to the FCM, implemented on a AMD Zynq-7030 SoC, which features a 28nm CMOS SRAM-based FPGA. Using the methodology described in Section III, we estimated the SEU rate for the FCM during the science phase of the mission.

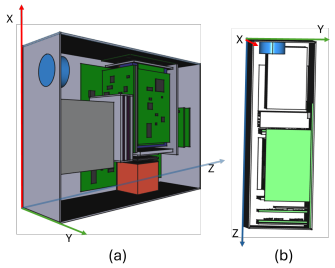


Fig. 2. Different view of CubeSat 3D Structure.

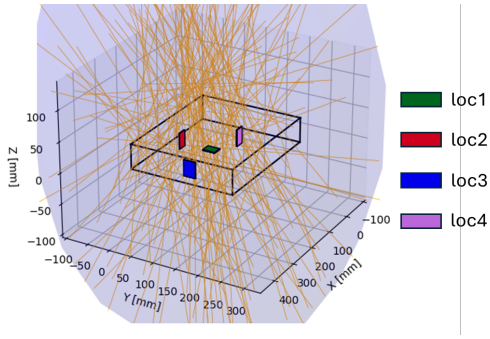


Fig. 3. Simplified view of target volume inside CubeSat. Each colored box refers to the same sensitive volume, located at different positions inside the CubeSat structure. Orange rays are just a visual representation of the radiation source geometry.

Using the SPENVIS platform, an interplanetary mission profile was configured with a 6-month duration, at a distance of 0.9 AU from the Sun, and under conditions of minimal solar activity. These inputs were derived from official trajectory and mission planning data. Once the mission environment was set, SPENVIS was used to compute the expected particle fluence. As the mission occurs during a solar minimum, the contribution of GCRs becomes dominant for SEE evaluation. Following this, the CubeSat geometry and the derived GCRs fluence are used as input for the GRAS engine. In GRAS, we modeled the particle source a 2.0 m diameter sphere emitting 10 million isotropic particles, incorporating the CubeSat. To emphasize the importance of 3D structural modeling in radiation effect evaluation, we evaluated the SEU rate for the FCM when placed in different feasible locations inside the CubeSat. As shown in Fig.3, the same chip is highlighted in different colors, each representing a distinct physical position within the satellite structure. In each case, the full PCB module containing the FCM was repositioned to a structurally realistic location. Although Fig. 3 presents a simplified model (intended for illustrative purposes), all subsystems and components not shown visually are still considered in the simulation and kept consistent across configurations. The output of GRAS is a dataset of LET spectra at the FCM for different location within the CubeSat. These spectra were then used as input to our custom analysis platform, which combines the LET data with the heavy-ion SEU cross-section of the Zynq-7000 device family [12]. The first set of experimental results, shown in Fig. 4, highlights the impact of incorporating the CubeSat's structural geometry into SEE rate estimation. Specifically,

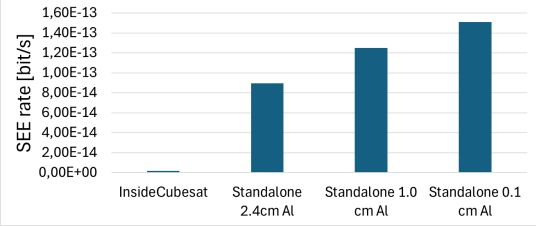


Fig. 4. SEE rate estimation for the FCM in different configurations.

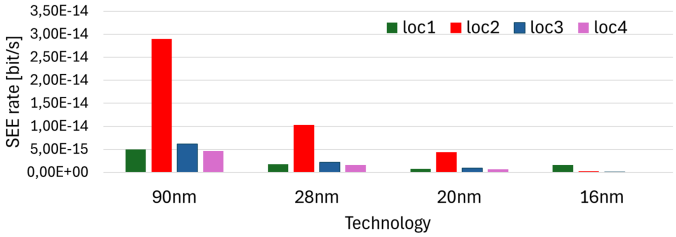


Fig. 5. SEE rate estimation considering different technologies and locations inside the CubeSat structure.

we compare the SEE rate calculated for the FCM in its nominal position (green in Fig. 3) with a baseline standalone estimation obtained from SPENVIS. Both evaluations use the same radiation environment model (i.e., GCR flux) and identical SEU cross-section data as input. However, the baseline relies on a simplified, uniform aluminum shielding model. The comparison reveals that structurally accurate evaluation predicts a SEE rate approximately 50 times lower than the most optimistic standalone case using 1.0 mm of aluminum shielding. This clearly demonstrates the significant risk of overestimation when relying solely on simplified shielding assumptions. The second set of experiments investigates how the SEE sensitivity of the same device varies with its physical placement within the CubeSat. Although the primary particle flux and device characteristics remain constant, the materials surrounding each location differ, influencing both nuclear interactions and the generation of secondary particles. To capture this, we performed SEU estimations for all chip placements shown in Fig.3. Additionally, to demonstrate the flexibility and generality of the proposed evaluation flow, we extended the analysis to assess the impact of the same LET spectra on devices manufactured using different technology nodes. This enables comparative analysis across technologies under a unified environmental and structural framework. This is feasible since the LET spectra are normalized per unit area (cm²), as is the SEU cross-section data for each technology. Given that, we use Heavy-Ions SEU cross-section data retrieved from [12] and [13], evaluating the effect of technology scaling from 90nm to 16nm. Results are shown in Fig. 5. For all locations, there is a clear decreasing trend in SEE rate as technology scales down from 90nm to 16nm. This is expected, as advanced nodes typically feature smaller sensitive volumes, reducing the probability of a high-energy particle causing a bit flip. The location of the chip inside the structure has a significant impact on the SEE rate. For example, loc2 consistently shows the highest SEE rate, especially for the 90nm case, where it reaches nearly 3e-14 bit/s, approximately 6× higher than loc1. This confirms the importance of accounting for local shielding and material composition, which affect the LET spectra due to secondary particles and scattering.

## V. Conclusion

We proposed an accurate SEE sensitivity evaluation flow through mission-specific 3D simulation. Experimental results show that it significantly improves the reliability and efficiency of CubeSat design. By capturing the impact of device placement and structural shielding, our methodology enables more realistic SEU rate predictions, supporting informed hardware selection and optimized fault mitigation strategies.

## Acknowledgment

The authors gratefully acknowledge Tyvak International and the European Space Agency (ESA) for the opportunity to contribute to the RAMSES mission study. Their support and collaboration have been essential in enabling this research.

## References

[1] P. E. Dodd, M. R. Shaneyfelt, J. R. Schwank and J. A. Felix, "Current and Future Challenges in Radiation Effects on CMOS Electronics," in IEEE Transactions on Nuclear Science, vol. 57, no. 4, pp. 1747-1763, Aug. 2010, doi: 10.1109/TNS.2010.2042613.

[2] D. S. Lee et al., "Single-Event Characterization of the 20 nm Xilinx Kintex UltraScale Field-Programmable Gate Array under Heavy Ion Irradiation," 2015 IEEE Radiation Effects Data Workshop (REDW), Boston, MA, USA, 2015, pp. 1-6, doi: 10.1109/REDW.2015.7336736.

[3] J. Allison et al., "Geant4 developments and applications," in IEEE Transactions on Nuclear Science, vol. 53, no. 1, pp. 270-278, Feb. 2006, doi: 10.1109/TNS.2006.869826.

[4] www.esa.int/Space_Safety/Planetary_Defence/Introducing_Ramses_ESA_s_mission_to_asteroid_Apophis

[5] E. G. Pereira et al., "Exploring Soft Error Susceptibility in FET Devices via Geant4 Simulation," 2025 IEEE 16th Latin America Symposium on Circuits and Systems (LASCAS), Bento Gonçalves, Brazil, 2025, pp. 1-5, doi: 10.1109/LASCAS64004.2025.10966230.

[6] K. Niskanen et al., "Proton Energy Dependence of SiC Power MOSFET Single-Event Burnout Sensitivity," in IEEE Transactions on Nuclear Science, vol. 72, no. 4, pp. 1412-1417, April 2025, doi: 10.1109/TNS.2025.3550609.

[7] D. Lambert et al., "Monte Carlo simulations: from neutron to defects in bulk materials," in IEEE Transactions on Nuclear Science, doi: 10.1109/TNS.2025.3554389.

[8] S. Hellmann et al., "CubeSat Concept for Demonstrating Efficient Directional Magnetic Radiation Protection for Spacecrafts Based on HTS Coils," in IEEE Transactions on Applied Superconductivity, vol. 35, no. 5, pp. 1-5, Aug. 2025, Art no. 3800305, doi: 10.1109/TASC.2025.3530333.

[9] [M. Kruglanski et al., "Last upgrades and development of the space environment information system (SPENVIS)," 2009 European Conference on Radiation and Its Effects on Components and Systems, Brugge, Belgium, 2009, pp. 563-565, doi: 10.1109/RADECS.2009.5994715.

[10] Santin, G. et al, GRAS: A general-purpose 3-D modular simulation tool for space environment effects analysis, IEEE Trans. Nucl. Sc., Vol 52, No 6, 2294-2299, 2005.

[11] E. Vacca et al.,"On Assessing the Robustness of RISC-V Soft Cores for Space Systems by Mission-Tailored SEU Analysis," 2024 31st IEEE International Conference on Electronics, Circuits and Systems (ICECS), Nancy, France, 2024, pp. 1-4, doi: 10.1109/ICECS61496.2024.10848907.

[12] V. Vlagkoulis et al., "Single Event Effects Characterization of the Programmable Logic of Xilinx Zynq-7000 FPGA Using Very/Ultra High-Energy Heavy Ions," in IEEE Transactions on Nuclear Science, vol. 68, no. 1, pp. 36-45, Jan. 2021.

[13] D. S. Lee et al., "Single-Event Characterization of 16 nm FinFET Xilinx UltraScale+ Devices with Heavy Ion and Neutron Irradiation," 2018 IEEE Radiation Effects Data Workshop (REDW), Waikoloa, HI, USA, 2018, pp. 1-8, doi: 10.1109/NSREC.2018.8584313.